Turbulent transport of toroidal angular momentum in fusion plasmas

I. Holod,[1] Z. Lin,[1,2] and Y. Xiao[1]
[1]*Department of Physics and Astronomy, University of California, Irvine, California 92697, USA*
[2]*Fusion Simulation Center, Peking University, Beijing 100871, China*

(Received 25 August 2011; accepted 14 December 2011; published online 26 January 2012)

Global nonlinear gyrokinetic simulations of ion temperature gradient (ITG) and collisionless trapped electron mode (CTEM) turbulence find significant spinning up of a plasma in the directions opposite for CTEM and ITG turbulence. The outward momentum convection by the particle flux could be strong enough to overcome the inward momentum pinch and reverse the radial direction of the convective momentum flux. Momentum pinch velocity shows no explicit dependence on background temperature, while it is significantly affected by steepening the background density. Convective momentum fluxes are generally smaller in the CTEM turbulence than the ITG turbulence, while the intrinsic Prandtl number is similar or slightly larger in the CTEM turbulence.
 [doi:10.1063/1.3677886]

I. INTRODUCTION

Plasma rotation plays an important role in turbulence stabilization,[1] transition to high confinement regime, and in the suppression of the resistive wall mode in the tokamak.[2] Hence, understanding momentum transport is crucial for achieving controlled thermonuclear fusion in magnetically confined plasmas. In the present day tokamaks, rotation is usually generated by applying external torque such as neutral beam injection. In the future larger machines like ITER,[3] the external momentum sources may not be adequate due to the significantly larger torque needed to spin up the plasma and due to the larger distance from the core to the edge, where external momentum is mostly deposited. This problem can possibly be solved by stimulating the inward transport of momentum through the momentum pinch[4–7] and by generating intrinsic torque driven by microturbulence.[8–10]

In general, the radial flux of toroidal angular momentum density (further referred to as momentum for simplicity) can be expanded into diffusive, convective, and residual components,

$$\Gamma_\phi = -\chi_\phi \partial_r L_\phi + V L_\phi + S,$$

where $L_\phi \equiv mRv_\phi$, R is the tokamak local major radius, v_ϕ is plasma toroidal velocity, and m is the ion mass ($m = 1$ in our normalization).

Convective and diffusive components of momentum flux are proportional to the momentum and momentum gradient, respectively. The convective flux directed inward is often referred to as a pinch. The leftover part of the momentum flux is usually called the residual stress. In our previous studies of the momentum transport using gyrokinetic particle simulation of the toroidal ion temperature gradient (ITG) turbulence with adiabatic[11] and kinetic electrons,[12] we have observed the existence of the momentum pinch and the intrinsic Prandtl number, defined as the ratio of momentum to the ion heat diffusivity, being smaller than unity. In this paper, we present the comparative studies of the toroidal momentum transport for two electrostatic turbulence regimes: collisionless trapped electron mode (CTEM) and ITG mode with kinetic electrons. All three components of the momentum flux have been studied one-by-one. In order to separate them, first, we run simulations of plasma with no background rotation. The momentum flux in this case is purely residual. Simulating plasma with rigid rotation provides the convective part, after subtracting the residual flux. Finally, considering sheared rotation case allows us to separate the diffusive component.

Radial transport of toroidal angular momentum has been simulated using the global nonlinear gyrokinetic code GTC.[13] The code is well benchmarked for simulating electrostatic drift-wave turbulence including ITG (Ref. 14) and CTEM.[15] In the simulations, ions dynamics is governed by gyroaveraged equations of motion,[16] and electrons are treated by a fluid-kinetic hybrid electron model.[17]

For the ITG case, the following parameters are used: $R_0/L_{Ti} = 4.5$, 6.9, 9.0, $R_0/L_{Te} = 0$, 2.2, and $R_0/L_n = 1.0$, 2.2, 4.5, where L_n is the density and $L_{Te/Ti}$ is the electron/ion temperature inhomogeneity scale length, and R_0 is the tokamak major radius. For the CTEM case, we use $R_0/L_{Ti} = 0$, 2.2, $R_0/L_{Te} = 4.5$, 6.9, 9.0, and $R_0/L_n = 1.0$, 2.2, 4.5. The tokamak minor radius is $a = 250\rho_i$, where ρ_i is the ion gyroradius. The toroidal rotation velocity and rotation shear are set to be small to minimize the effect of rotating plasma on the underlying turbulence. To illustrate that we plot in Fig. 1 the time history of the electron heat conductivity χ_e for three toroidal rotation frequencies: $\omega_\phi = 0$, $\omega_\phi = 0.075 v_i/R_0$, and $\omega_\phi = (0.05 - 0.1r/a)v_i/R_0$, where v_i is the ion thermal velocity, and r is the local minor radius of the tokamak. The saturated value of χ_e remains practically the same for all three frequencies, which indicates that the rotations do not significantly affect the background turbulence.

II. INTRINSIC ROTATION: RESIDUAL FLUX

The typical radial profiles of the toroidal angular momentum after nonlinear saturation in a plasma with no background rotation are shown in Figs. 2 and 3 for the case of CTEM and ITG turbulence, respectively. As we can see,

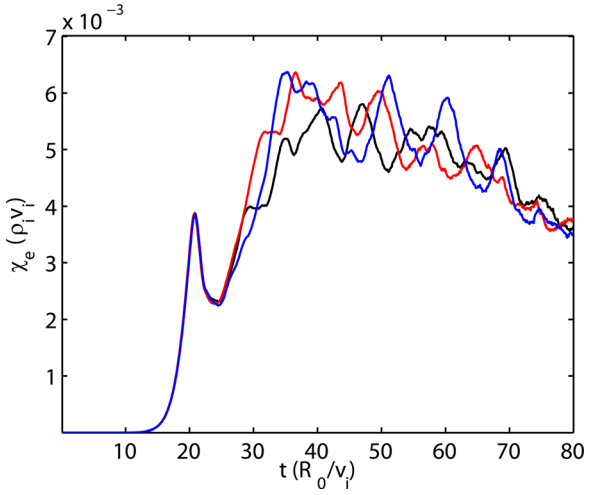

FIG. 1. (Color online) Time evolution of electron heat conductivity for CTEM-I case. Angular frequency of background rotation is $\omega_\phi = 0$ (black line), $\omega_\phi = 0.075 v_i/R_0$ (red line), and $\omega_\phi = (0.05 - 0.1 r/a) v_i/R_0$ (blue line).

plasma rotation is redistributed within the radial simulation domain, with the volume averaged value staying close to zero. Momentum flux through the boundaries is zero, since all fluctuations are suppressed in the near-boundary region.

We observe that rotation direction in corresponding radial locations is opposite in the CTEM and ITG turbulence, leading to the negative (counter-current) spinning up of the plasma core in the CTEM case and positive (co-current) spinning up in the ITG case. It turns out that plasma rotation is well correlated with the self generated radial electric field $-\partial_r \phi_{00}$, shown in dashed line in Figs. 2 and 3, where ϕ_{00} is zonal component of the electrostatic potential. Possible explanation could be the partial relaxation to neoclassical state, with turbulence acting as an effective collision operator.

Radial profiles of the normalized residual momentum fluxes are shown in Figs. 4 and 5 for the CTEM and ITG turbulences. In the same figures, we plot normalized profiles of self generated radial electric field shear multiplied by turbulence intensity, $I\partial_r^2 \phi_{00}$ (taken with negative sign in Fig. 5). Correlation between momentum fluxes and E_r-shear suggests

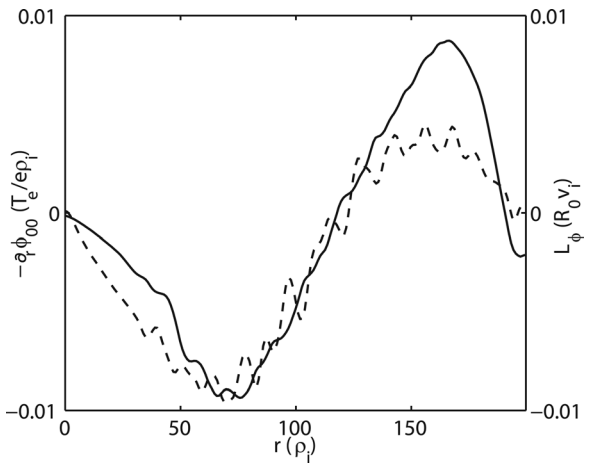

FIG. 2. Time-averaged radial profiles of toroidal angular momentum (solid line) and self generated radial electric field (dashed line). CTEM case with $R_0/L_{Ti} = 2.2$, $R_0/L_{Te} = 6.9$, and $R_0/L_n = 2.2$.

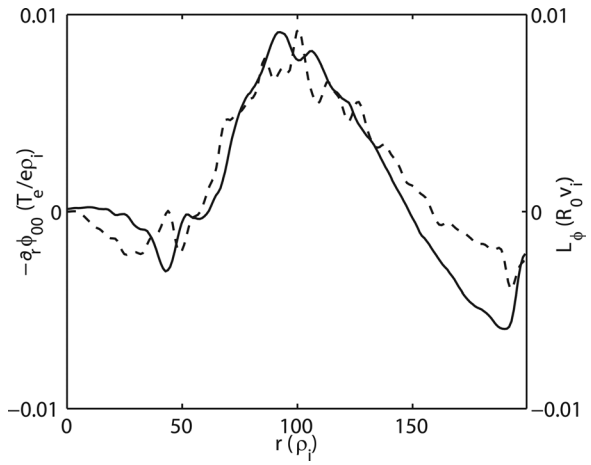

FIG. 3. Time-averaged radial profiles of toroidal angular momentum (solid line) and self generated radial electric field (dashed line). ITG case with $R_0/L_{Ti} = 6.9$, $R_0/L_{Te} = 2.2$, and $R_0/L_n = 2.2$.

that zonal $E \times B$ shear provides the necessary symmetry breaking mechanism to drive the residual momentum flux.[18] The fact that radial profiles of self-generated electric field are similar but inverted in the CTEM and ITG cases is compensated by negative sign in the momentum flux proportionality to the E_r-shear, leading to the similar profiles for momentum fluxes in both CTEM and ITG turbulence. This observation suggests that the residual momentum flux plays minor role in establishing the perturbed toroidal momentum profile which seems to be directly determined by the zonal flow structure.

III. CONVECTIVE FLUX

Convective flux of the toroidal angular momentum is obtained by running simulations with constant angular frequency, after subtraction of the residual flux S. The convective flux is then separated into a particle convection and a momentum pinch,

$$\Gamma_{\text{conv}} = \frac{1}{n}\Gamma_n L_\phi + V_\phi L_\phi,$$

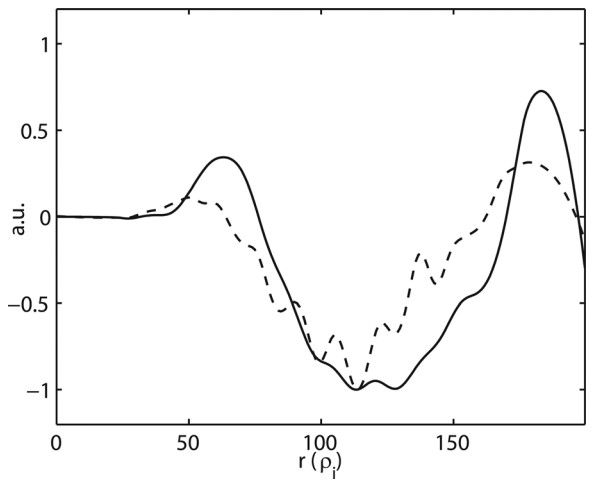

FIG. 4. Time-averaged normalized radial profiles of toroidal angular momentum flux (solid line) and self generated radial electric field shear (dashed line). CTEM case with $R_0/L_{Ti} = 2.2$, $R_0/L_{Te} = 6.9$, and $R_0/L_n = 2.2$.

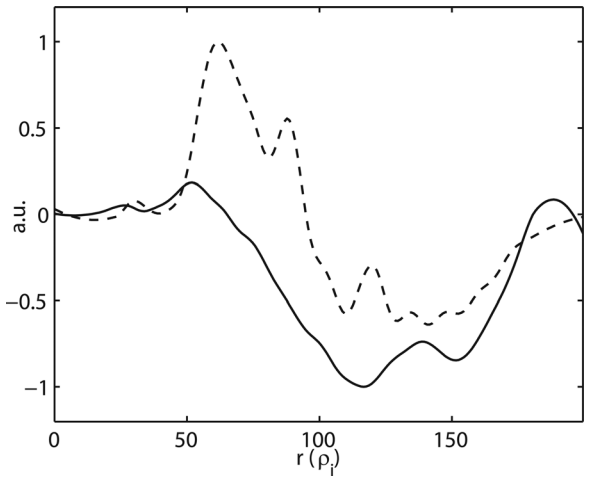

FIG. 5. Time-averaged radial profiles of toroidal angular momentum flux (solid line) and self generated negative radial electric field shear (dashed line). ITG case with $R_0/L_{Ti}=6.9$, $R_0/L_{Te}=2.2$, and $R_0/L_n=2.2$.

where Γ_n is the particle flux, and V_ϕ is the momentum pinch velocity.

Particle convection, mainly determined by the density gradient, is typically outward in our simulations, while the momentum pinch usually has radially inward direction.[11,19,23] We observe the particle convective flux to be relatively small in the ITG case (Fig. 6(a)) and much more pronounced in the CTEM cases (Figs. 6(b) and 6(c)). In the case of large density gradient, the particle convection is able to overturn the momentum pinch and switch the direction of the resulting momentum convective flux from inward to outward (Fig. 6(c)).

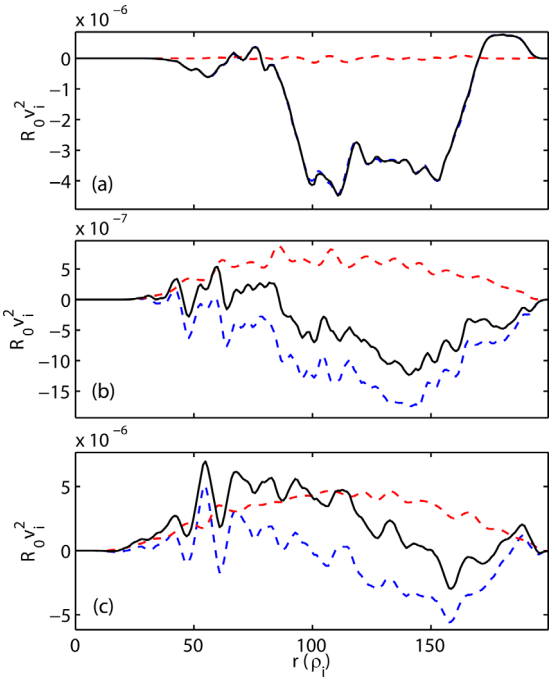

FIG. 6. (Color online) Time-averaged radial profiles of momentum pinch flux (dashed blue line), momentum convected by particle flux (dashed red line), and total momentum flux (solid black line). Panel (a): ITG case with $R_0/L_{Ti}=4.5$, $R_0/L_{Te}=0$, and $R_0/L_n=1$. Panel (b): CTEM case with $R_0/L_{Ti}=0$, $R_0/L_{Te}=4.5$, and $R_0/L_n=1$. Panel (c): CTEM case with $R_0/L_{Ti}=0$, $R_0/L_{Te}=4.5$, and $R_0/L_n=4.5$. Angular frequency of rigid rotation is $\omega_\phi=0.075v_i/R_0$ for all cases.

TABLE I. Equilibrium parameter dependence of convective momentum fluxes. Momentum convection velocity is shown in v_i units. Turbulence intensity, I, is normalized by T_e^2/e^2, and heat conductivity (ion for ITG cases and electron for CTEM cases) χ is normalized by v_iT_e.

R_0/L_{Ti}	R_0/L_{Te}	R_0/L_n	$V_\phi/I\times10^2$	$\frac{1}{n}\Gamma_n/I\times10^2$	$V_\phi/\chi\times10^3$
			ITG		
9.0	0	1.0	-20.1 ± 3.0	0.1 ± 0.1	-1.2 ± 0.2
9.0	0	2.2	-16.1 ± 4.1	0.7 ± 0.1	-1.0 ± 0.2
9.0	0	4.5	-5.8 ± 3.9	3.9 ± 0.4	-0.5 ± 0.3
4.5	0	1.0	-22.0 ± 6.4	0.0 ± 0.1	-1.5 ± 0.4
4.5	0	2.2	-16.9 ± 4.7	0.7 ± 0.2	-1.2 ± 0.4
			CTEM		
0	9.0	1.0	-6.0 ± 1.1	3.2 ± 0.3	-5.6 ± 1.4
0	9.0	2.2	-5.6 ± 1.2	4.4 ± 0.7	-4.4 ± 1.1
0	9.0	4.5	-4.1 ± 2.4	6.8 ± 1.5	-2.9 ± 1.6
0	4.5	1.0	-5.8 ± 1.2	3.2 ± 0.3	-6.2 ± 1.1
0	4.5	2.2	-4.6 ± 1.7	4.1 ± 0.6	-4.0 ± 1.6

We have studied the dependence of the momentum convective flux on the scale lengths of plasma density and temperature inhomogeneity. To eliminate the direct effect of background inhomogeneities as a turbulence drive, the momentum fluxes are normalized by turbulence intensity. Corresponding simulation results are presented in Table I. Two cases, one near and one far from marginality are considered for the ITG and CTEM turbulence. As we can see from the Table I, there is practically no explicit dependence on the equilibrium plasma temperature inhomogeneity scale-length observed for a given turbulence regime.

When the density gradient is increasing, we observe significant decreasing of the momentum pinch velocity and, naturally, increasing of the particle convective flux.

Since ion transport is diffusive in both ITG (Ref. 22) and CTEM turbulence[15] due to the parallel wave-particle decorrelation,[20,21] the momentum pinch is simply off-diagonal elements of the viscosity tensor.

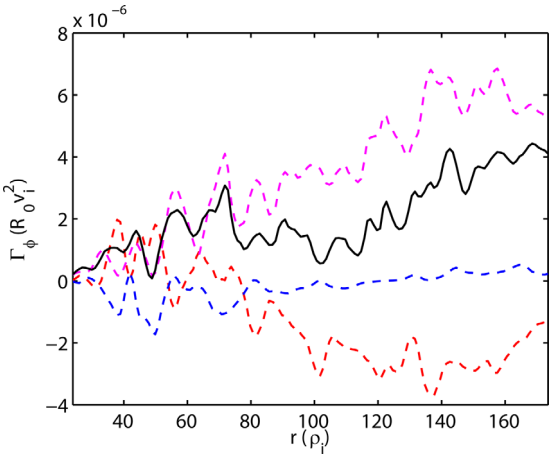

FIG. 7. (Color online) Time-averaged radial profiles of residual momentum flux (dashed red line), convective momentum flux (dashed blue line), diffusive momentum flux (dashed green line), and total momentum flux (solid black line). CTEM case with $R_0/L_{Ti}=2.2$, $R_0/L_{Te}=6.9$, and $R_0/L_n=2.2$. Angular frequency of sheared rotation is $\omega_\phi=(0.05-0.1r/a)v_i/R_0$.

To summarize, the convective momentum flux obtained in the rigid rotation case consists of inward pinch and particle convective flux. Strong outward particle flux, often more pronounced in the CTEM turbulence, can lead to the reversal of the momentum convective flux. The overall momentum convection is smaller in the CTEM turbulence compared to the ITG turbulence.

IV. DIFFUSIVE FLUX

The diffusive momentum flux is obtained by simulating plasma with sheared background rotation and subtracting the residual and convective momentum fluxes,

$$\Gamma_{\text{diff}} \equiv -\chi_\phi \partial_r L_\phi = \Gamma_\phi - \Gamma_{\text{conv}} - S.$$

The background rotation profile is constructed in a way that there is zero angular frequency in the middle of the radial domain to minimize the convective component. Corresponding angular frequency is chosen as $\omega_\phi = (0.05 - 0.1r/a)v_i/R_0$.

Using the obtained diffusive flux, we have calculated the ratio of momentum diffusivity to ion heat conductivity, referred to as an intrinsic Prandtl number, $\text{Pr} \equiv \chi_\phi/\chi_i$. The Prandtl number is undetermined for previously considered CTEM cases with flat ion temperature, since χ_i becomes infinite. For the ITG and CTEM cases with finite ion and electron temperature gradient, we have found $\text{Pr}_{\text{CTEM}} = 1.0$, for the CTEM turbulence ($R_0/L_{Ti} = 2.2$, $R_0/L_{Te} = 6.9$, and $R_0/L_n = 2.2$) and $\text{Pr}_{\text{ITG}} = 0.7$ for the ITG mode turbulence ($R_0/L_{Ti} = 6.9$, $R_0/L_{Te} = 2.2$, and $R_0/L_n = 2.2$).

The example of the structure of toroidal momentum flux for the CTEM turbulence is shown in Fig. 7, where we plot the time-averaged radial profiles of the residual (dashed red line), convective (dashed blue line), diffusive (dashed green line), and total (solid black line) toroidal momentum fluxes. For a given rotation profile, $\omega_\phi = (0.05 - 0.1r/a)v_i/R_0$, diffusive flux is dominant. The residual flux can be comparable to the total flux locally, but it is generally smaller after volume averaging. Momentum convection is negligible, since the volume averaged angular frequency is chosen to be zero.

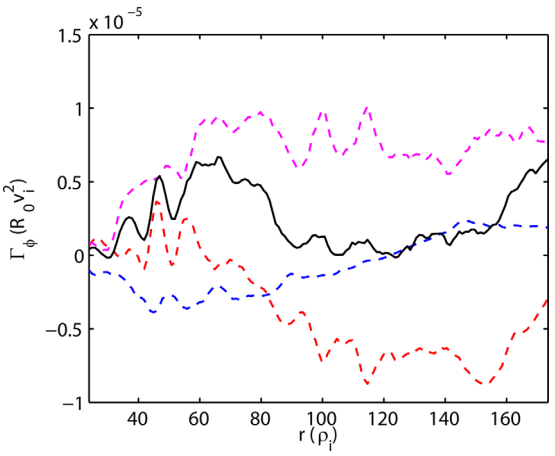

FIG. 8. (Color online) Time-averaged radial profiles of residual momentum flux (dashed red line), convective momentum flux (dashed blue line), diffusive momentum flux (dashed green line), and total momentum flux (solid black line). ITG case with $R_0/L_{Ti} = 6.9$, $R_0/L_{Te} = 2.2$, and $R_0/L_n = 2.2$. Angular frequency of sheared rotation is $\omega_\phi = (0.05 - 0.1r/a)v_i/R_0$.

The picture similar to CTEM is observed in the case of ITG turbulence (Fig. 8).

V. CONCLUSIONS

We have addressed the physics of the toroidal angular momentum transport in the ITG and CTEM turbulence regimes. Starting with no background rotation, we observe significant spinning up of a plasma after turbulence saturation. The direction of this intrinsic rotation is opposite in corresponding radial domains in the CTEM and ITG turbulence.

Simulating plasma with constant background toroidal angular velocity, we have found that with the sufficiently large density gradient, particle convective momentum flux can successfully compete with the inward pinch, resulting in the reversal of the total momentum convective flux, especially in the CTEM turbulence regime. The dependencies of the momentum convective flux on background plasma temperature and density gradients show that the increase of the temperature gradient leads to the increase of turbulence intensity, which means stronger momentum convection. When momentum pinch is normalized by turbulence intensity, there is no explicit dependence of the temperature gradient scale length observed for a given turbulence regime. In turn, steepening of the background density gradient leads to decreasing of the momentum pinch, most significantly near the turbulence marginality.

Separation of different components of the momentum flux allows us to calculate the momentum diffusivity and the intrinsic Prandtl number, which is found to be close to unity and slightly larger in the CTEM turbulence, compared to the ITG mode turbulence.

ACKNOWLEDGMENTS

The authors acknowledge useful discussions with Liu Chen and Taik-Soo Hahm. This work was supported by U.S. Department of Energy Plasma Science Center, SciDAC GPS and GSEP centers, and INCITE programs. Simulations were performed on supercomputers at NCCS and NERSC.

[1]K. H. Burrell, Phys. Plasmas **4**, 1499 (1997).
[2]D. J. Ward and A. Bondeson, Phys. Plasmas **2**, 1570 (1995).
[3]See http://www.iter.org for the detailed description of the ITER project.
[4]K. Nagashima, Y. Koide, and H. Shirai, Nucl. Fusion **34**, 449 (1994).
[5]M. Yoshida, Y. Koide, H. Takenaga, H. Urano, N. Oyama, K. Kamiya, Y. Sakamoto, G. Matsunaga, Y. Kamada, and the JT60 Team, Nucl. Fusion **47**, 856 (2007).
[6]W. M. Solomon, S. M. Kaye, R. E. Bell, B. P. Leblanc, J. E. Menard, G. Rewoldt, W. Wang, F. M. Levinton, H. Yuh, and S. A. Sabbagh, Phys. Rev. Lett. **101**, 065004 (2008).
[7]T. Tala, K. D. Zastrow, J. Ferreira, P. Mantica, V. Naulin, A. G. Peeters, G. Tardini, M. Brix, G. Corrigan, C. Giroud, and D. Strintzi, Phys. Rev. Lett. **102**, 075001 (2009).
[8]K. Ida, Phys. Rev. Lett. **74**, 1990 (1995).
[9]K. Ida, J. Phys. Soc. Jpn. **67**, 4089 (1998).
[10]W. M. Solomon, K. H. Burrell, J. S. deGrassie, R. Budny, R. J. Groebner, J. E. Kinsey, G. J. Kramer, T. C. Luce, M. A. Makowski, D. Mikkelsen, R. Nazikian, C. C. Petty, P. A. Politzer, S. D. Scott, M. A. Van Zeeland, and M. C. Zarnstorff, Plasma Phys. Controlled Fusion **49**, B313 (2007).
[11]I. Holod and Z. Lin, Phys. Plasmas **15**, 092302 (2008).
[12]I. Holod and Z. Lin, Plasma Phys. Controlled Fusion **52**, 035002 (2010).
[13]Z. Lin, T. S. Hahm, W. W. Lee, W. M. Tang, and R. B. White, Science **281**, 1835 (1998).

[14]Z. Lin, T. S. Hahm, S. Ethier, and W. M. Tang, Phys. Rev. Lett. **88**, 195004 (2002).
[15]Y. Xiao and Z. Lin, Phys. Rev. Lett. **103**, 085004 (2009).
[16]W. W. Lee, Phys. Fluids **26**, 556 (1983).
[17]I. Holod, W. L. Zhang, Y. Xiao, and Z. Lin, Phys. Plasmas **16**, 122307 (2009).
[18]O. D. Gurcan, P. H. Diamond, T. S. Hahm, and R. Singh, Phys. Plasmas **14**, 042306 (2007).
[19]T. S. Hahm, P. H. Diamond, O. D. Gurcan, and G. Rewoldt, Phys. Plasmas **14**, 072302 (2007).
[20]I. Holod and Z. Lin, Phys. Plasmas **14**, 032306 (2007).
[21]Z. Lin, I. Holod, L. Chen, P. H. Diamond, T. S. Hahm, and S. Ethier, Phys. Rev. Lett. **99**, 265003 (2007).
[22]W. L. Zhang, Z. Lin, and L. Chen, Phys. Rev. Lett. **101**, 095001 (2008).
[23]A. G. Peeters, C. Angioni, and D. Strintzi, Phys. Rev. Lett. **98**, 265003 (2007).